Wavelength-Dependent Ultrafast Charge Carrier Separation in the $WO_3/BiVO_4$ Coupled System

Ivan Grigioni,[†] Kevin G. Stamplecoskie,[‡] Danilo H. Jara,[§] Maria Vittoria Dozzi,[†] Aurelio Oriana,[∥] Giulio Cerullo,[∥] Prashant V. Kamat[§] and Elena Selli*[,†]

[†] Dipartimento di Chimica, Università degli Studi di Milano, Via Golgi 19, I-20133 Milano, Italy

[‡] Department of Chemistry, Queen's University, Kingston, Ontario K7L 3N6, Canada

[§] Radiation Laboratory, University of Notre Dame, Notre Dame, Indiana 46556, United States

[∥] IFN-CNR, Department of Physics, Politecnico di Milano, Piazza Leonardo da Vinci 32, I-20133 Milano, Italy

Table of content

1. Experimental

1.1. Materials

The following chemicals were employed: tungsten(VI) ethoxide 99.8% (5% w/v in ethanol), ammonium vanadium oxide, bismuth(III) nitrate pentahydrate 98%, benzyl alcohol 99% (Alpha Aesar); ethyl cellulose, citric acid 99% (Aldrich); anhydrous sodium sulfate (Fisher Scientific).

1.2. Photoelectrodes preparation

WO_3 was prepared as described in our previous work.[1] Briefly, 1.0 mL of tungsten ethoxide, 5 wt.% in ethanol, was added inside a glovebox to 42 mg of citric acid acting as stabilizer. Once citric acid was completely dissolved, benzyl alcohol (0.3 mL) and ethyl cellulose (40 mg) were added to the solution, which was stirred overnight at 70° C to attain complete ethyl cellulose dissolution. The so obtained paste (with a 0.085 M tungsten content) is stable for several weeks. 100 µL of the paste were deposited on a 2.5 x 2.5 cm^2 fluorine-doped tin oxide (FTO) glass electrode (Pilkington Glass, TEC-7, thickness 2 mm), by spin coating at 6000 rpm for 30 s. The final spinning rate was reached with a three acceleration step program, *i.e.* 500 rpm s^{-1} up to 1000 rpm, then 1000 rpm s^{-1} up to 3000 rpm and finally 3000 rpm s^{-1} up to 6000 rpm. Prior to deposition, the FTO glass was cleaned by 15 min-long sonication, first in an aqueous soap solution, then in ethanol and finally in water. After coating, the so obtained film was dried at 80 °C for 1 h and then annealed at 500 °C for 8 h.

The $BiVO_4$ (BV) films were prepared according to a procedure similar to that reported elsewhere.[2] Typically, 0.002 mol of $Bi(NO_3)_3$ and NH_4VO_3 were added to 6 mL of HNO_3 23.3% containing 0.004 mol of citric acid. The mixture was stirred overnight to allow the complete dissolution of all precursors. The $BiVO_4$ based photoanodes were prepared on

clean FTO by spinning 70 µL of the solution at 8000 rpm for 30 s with an acceleration rate of 6000 rpm s^{-1}. The films were then dried at 80 °C for 1 h and annealed at 500 °C for 1 h. The optical density of the $BiVO_4$ layer was modulated by repeating the spin coating procedure and the thermal treatment up to four times; then the photoelectrodes were annealed at 500 °C for 8 h.

The $WO_3/BiVO_4$ (WBV) combined films were prepared by coating WO_3 electrodes with the solution containing the $BiVO_4$ precursors. Then the composite films were dried for 1 h at 80 °C and annealed at 500 °C for 1 h. The process was repeated four times and the final films were annealed at 500 °C for 8 h.

1.3. Photoelectrodes characterization

Images showing the morphology and the cross section view of the electrodes were obtained using a FEI Magellan-400 field emission scanning electron microscope (FESEM). UV-visible absorption spectra, also under an applied bias, were recorded using a Jasco V650 spectrophotometer. The crystalline phase of the materials was determined through XRPD analysis using a Philips PW1820 with Cu K_α radiation (λ = 1.54056 Å) at 40 mA and 40 kV.

1.4. Photoelectrochemical (PEC) characterization

PEC measurements were carried out using a three electrode cell with an Ag/AgCl (3.0 M NaCl) reference electrode, a platinum gauze as a counter electrode and a Princeton Applied Research 2263 (PARstat) potentiostat. The photoanodes were tested under back side illumination (through the $FTO/BiVO_4$ or $FTO/WO_3/BiVO_4$ interface). The light source was an Oriel, Model 81172 solar simulator providing AM 1.5G simulated solar illumination with 100 mW cm^{-2} intensity (1 sun). A 0.5 M Na_2SO_4 aqueous solution at pH

= 7 was used in electrochemical measurements. The potential *vs.* Ag/AgCl was converted into the RHE scale using the following equation: $E_{RHE} = E_{AgCl} + 0.059\ pH + E^{o}_{AgCl}$, with E^{o}_{AgCl} (3.0 M NaCl) = 0.210 V at 25°C.

Incident photon to current efficiency (IPCE) measurements were carried out using a 300 W Lot-Oriel Xe lamp equipped with a Lot-Oriel Omni-λ 150 monochromator and a Thorlabs SC10 automatic shutter. A 1.23 V bias *vs.* NHE was applied and the current was measured with a 10 nm step, within the 350 to 600 nm wavelength range. The incident light power was measured at each wavelength using a calibrated Thorlabs S130VC photodiode connected to a Thorlabs PM200 power meter. Typical values are reported in Figure S1. The IPCE was calculated at each wavelength using the following equation:

$$IPCE = \frac{[1240\ \times J]}{P}$$

where J is the photocurrent density (mA cm^{-2}) and P_{λ} (mW cm^{-2}) is the power of the monochromatic light at wavelength λ (nm).

The internal quantum efficiency (IQE) was calculated by combining the IPCE spectrum with the absorption (A) spectrum of the photoanodes:[3]

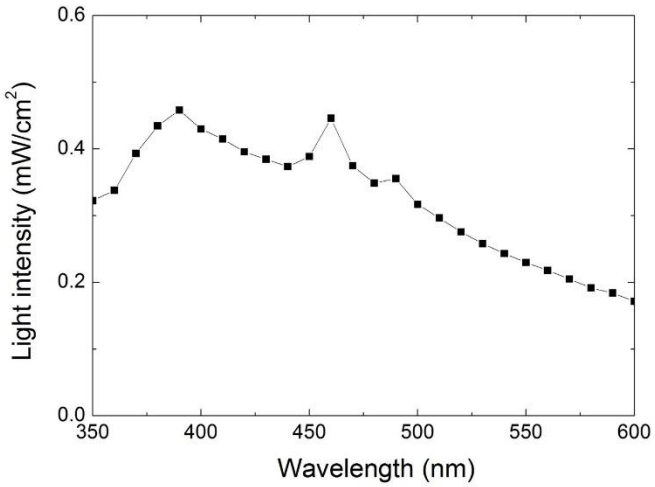

Figure S1. Light intensity typically employed in our IPCE measurements.

1.5. Transient absorption spectroscopy

Femtosecond transient absorption (TA) experiments with 387 nm laser pulse excitation were performed at the Radiation Laboratory, Notre Dame University, using a system based on a Ti:sapphire laser source (Clark MXR CPA-2010) generating pulses centered at 775 nm with a FWHM of 130 fs and 1 kHz repetition rate; 95% of the fundamental laser pulse was frequency doubled to λ = 387 nm and used as pump, while the remaining 5% was focused on a CaF_2 crystal to generate the white light continuum (WLC) probe. The transient spectra were recorded using a Helios transient absorption system of Ultrafast Systems. Pump energy fluences ranging from 20 to 120 μJ cm^{-2} were employed during the experiments with excitation at 387 nm.

Femtosecond TA experiments with tunable excitation wavelength were performed at the Department of Physics, Politecnico di Milano, using an amplified Ti:sapphire laser system (Libra, Coherent) delivering 4 mJ, 100 fs pulses at 800 nm with 1 kHz repetition

rate. Wavelength tunable pump pulses were generated by an optical parametric amplifier (OPA) pumped by the second harmonic of the laser and seeded by a WLC produced in a sapphire plate.[4,5] The OPA produced ≈ 70 fs pulses tunable between 480 and 1050 nm, that were used directly as the pump (500 nm) or frequency doubled, in the case of 460 and 450 nm pumps. Similar to the previous setup, a portion of the laser output was focused on a CaF_2 plate to generate a WLC used as broadband probe. TA spectra were measured with a spectrometer (Acton Sp2150, Princeton Instruments) equipped with a CCD camera (Entwicklungsbro Stresing) detecting data at the full 1 kHz repetition rate of the laser. Pump energies of 50 and 1000 nJ per pulse (corresponding to an intensity of 250 and 5000 μJ cm^{-2}) were used for the 450 and 460 nm pumps, and for the 500 nm pump, respectively, in order to obtain comparable photoexcitation densities at the different wavelengths used.

2. Estimation of the thickness of the $BiVO_4$ layer

We performed a SEM cross sectional analysis of the samples and calculated the thickness of the BV and WO_3 layer by subtracting the average thickness of the FTO layer from the average thickness of the FTO/BV and FTO/WO_3 layer (obtained from Figure S2A, B and C, respectively). We estimated the thickness of the $BiVO_4$ film in the WBV electrode by subtracting the thickness of the FTO/WO_3 layer from that of the FTO/WO_3/$BiVO_4$ multilayer (calculated from Figure S2D).

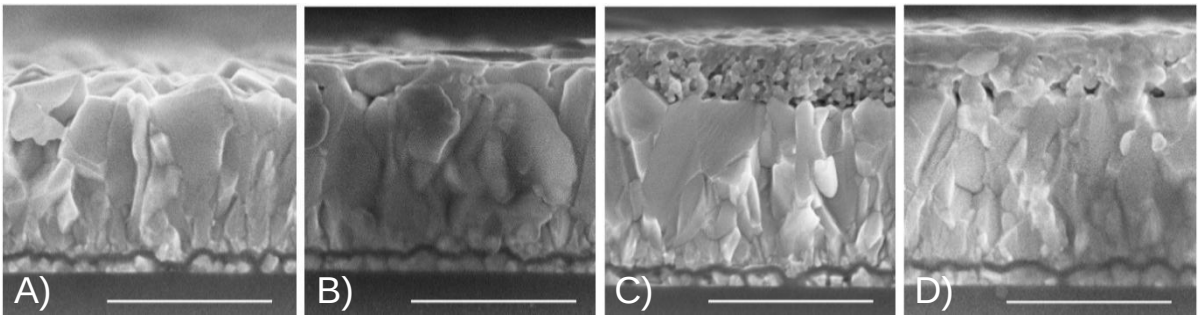

Figure S2. Cross section FESEM images of (A) clean FTO, (B) BV, (C) WO_3, and (D) WBV. The scale bar is 500 nm.

3. XRPD analysis

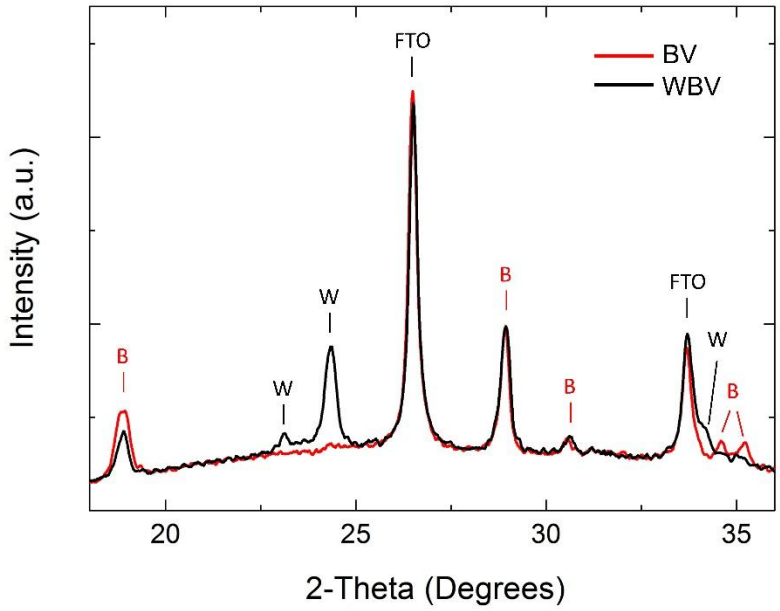

Figure S3. XRPD analysis of the BV (red trace) and WBV (black trace) electrodes in the 18 – 36° region. The typical peaks ascribed to $BiVO_4$ monoclinic scheelite, WO_3 monoclinic structure as well as those of FTO are labeled with B, W and FTO, respectively. Each photoanode was annealed 8 h at 500 °C.

4. Transient photobleaching

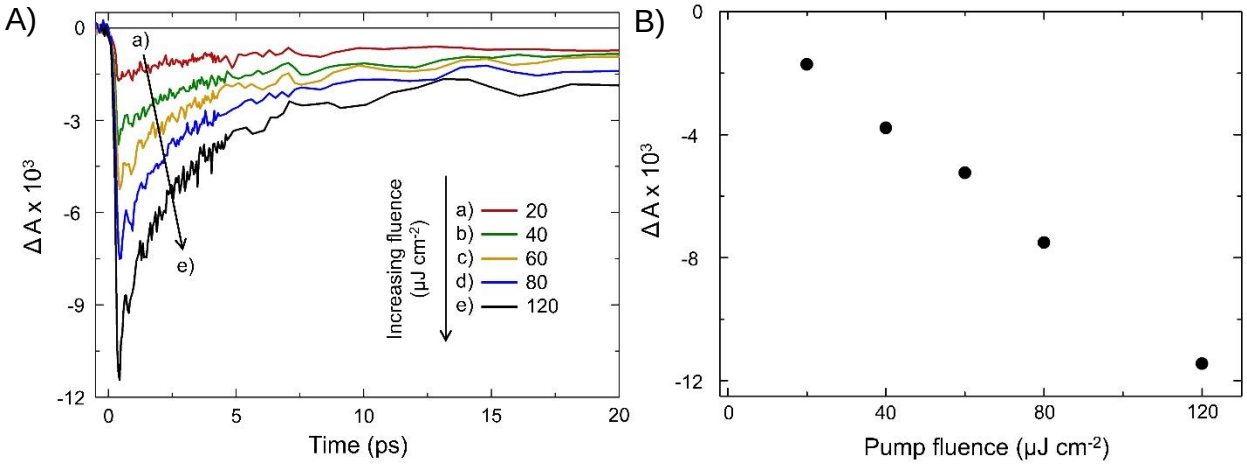

Figure S4. (A) TA time traces recorded at 420 nm with the BV film upon excitation at 387 nm with a (a) 20, (b) 40, (c) 60, (d) 80, and (e) 120 μJ cm^{-2} fluence. (B) Correlation between the maximum transient photobleaching ΔA at 420 nm and the used pump fluence.

5. Trapped hole dynamics in $BiVO_4$

The trapped hole dynamics in photoexcited $BiVO_4$ has been investigated by Ravensberger et al. and is sketched in Figure S5.[6]

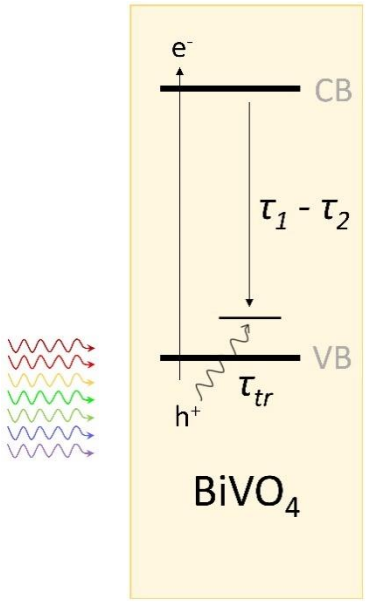

Figure S5. Diagram of the charge carrier transitions occurring upon excitation of $BiVO_4$. First, holes diffuse to and get trapped at surface trap states (τ_{tr}); then trapped holes recombine with electrons, according to a bi-exponential decay (τ_1 and τ

6. Buildup of the Δ*A* signal at 470 nm

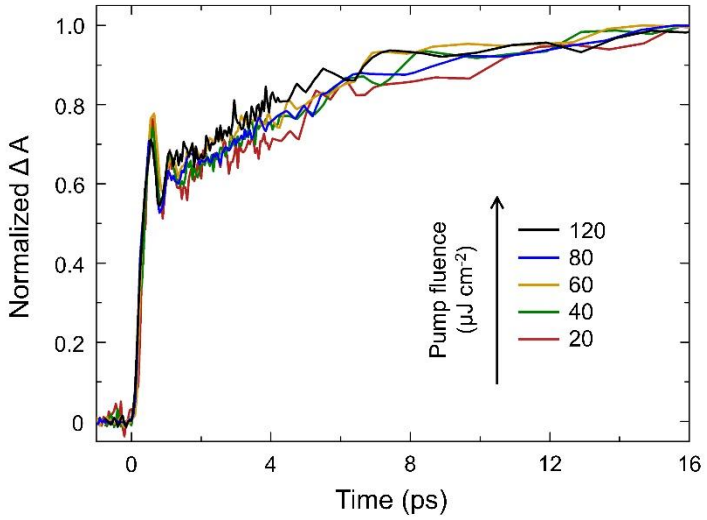

Figure S6. Normalized Δ*A* buildup in BV recorded at 470 nm for different pump fluences.

7. Transient absorption profiles, curve fitting and fitting parameters

Figure S7 highlights the contribution to the Δ*A* time evolution of the trapped holes signal in $BiVO_4$ of each of the processes described in Figure S5; the fitting curve obtained by eq 1 is reported in red.

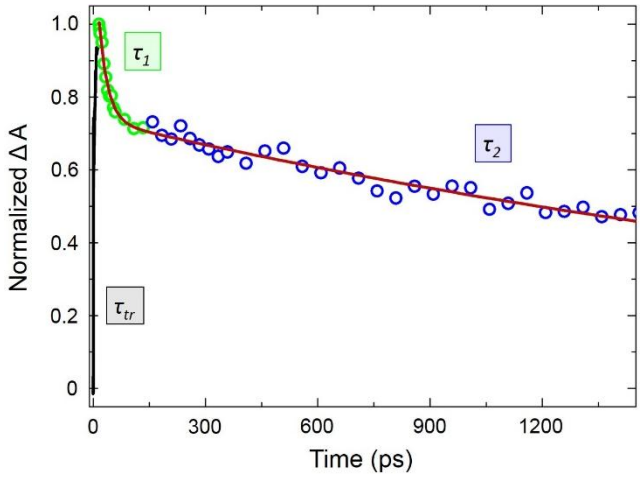

Figure S7. Normalized TA time trace recorded at 470 nm upon excitation of the BV photoanode with the 387 nm pump (40 μJ cm^{-2}). The three processes responsible for the Δ*A* time evolution are highlighted with different colors on the decay profile. The fitting trace obtained by fitting the decay with eq 1 is reported in red.

Table S1. Fitting parameters according to eq 1 of the Δ*A* transient decays recorded at 470 nm after excitation of a BV film at 387 nm with different pump fluences.

	Pump fluence (μJ cm^{-2})				
	20	**40**	**60**	**80**	**120**
A_1	0.34 ± 0.01	0.27 ± 0.01	0.28 ± 0.01	0.26 ± 0.01	0.24 ± 0.02
τ_1 (ps)	26 ± 2	24 ± 2	28 ± 3	15 ± 2	17 ± 2
A_2	0.66 ± 0.01	0.73 ± 0.01	0.72 ± 0.01	0.74 ± 0.01	0.77 ± 0.01
τ_2 (ns)	2.87 ± 0.15	3.06 ± 0.13	3.09 ± 0.16	3.04 ± 0.11	2.56 ± 0.10

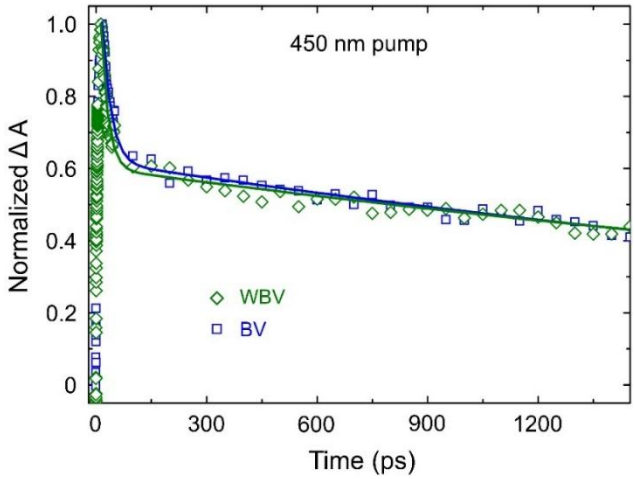

Figure S8. Normalized TA time trace at 470 nm of the BV and WBV films upon excitation with a 450 nm pump. The evolution of the Δ*A* signals due to holes trapped in the two systems is similar.

Similar to Figure S7, Figure S9 highlights the growth and the three decay processes occurring in the WBV coupled system and reports in red the fitting curve obtained by eq 2. Compared to Figure S7, the further exponential decay process ascribed to the injection of electrons from the CB of WO_3 to the VB of $BiVO_4$ (see Figure 6 in the main text) leads to a faster Δ*A* decay. The τ_{tr} process partially overlaps with τ_1 and fades out during the first 200 ps of τ_2.

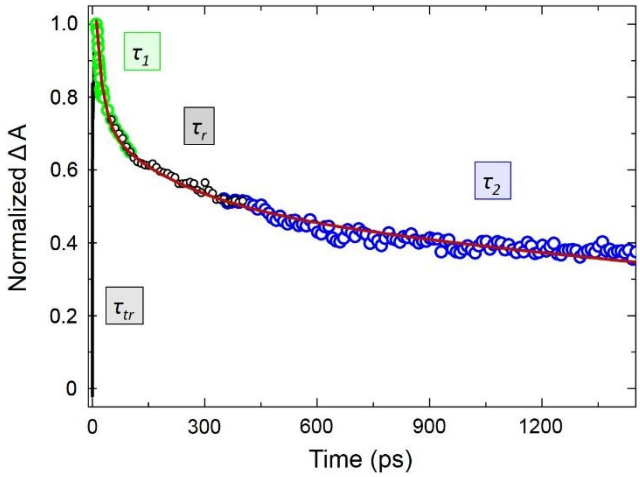

Figure S9. Normalized TA time trace at 470 nm upon excitation of the WBV photoanode at 387 nm (40 μJ cm^{-2}). The four processes responsible for Δ*A* evolution are highlighted with different colors. The fitting trace obtained by fitting the decay with eq 2 is reported in red.

8. Integration of the IPCE spectrum of WBV

We integrated the IPCE curve of the WBV photoanode (trace 1 in Figure 5B) over the AM 1.5G reference solar spectrum and the obtained photocurrent density of 0.99 mA cm^{-2} well correlates with the value of 0.87 mA cm^{-2} recorded at 1.23 V *vs.* RHE during the sweep voltammetry experiment reported in Figure 5A.[7] The good agreement confirms that the recombination of photogenerated e^{-}–h^{+} couples is not affected by the incident light fluence. The small difference between the two values can be ascribed to the spectral mismatch between the AM 1.5G spectrum and the emission spectrum of the light source employed in PEC measurements.

9. Swept IPCE under 350 and 450 nm irradiation

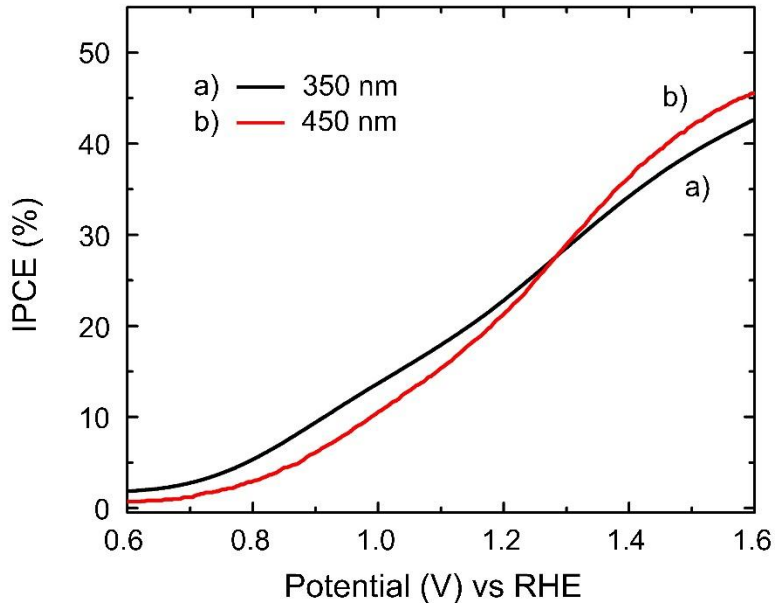

Figure S10. Swept IPCE measured by biasing a WBV photoanode from 0.6 to 1.6 V *vs.* RHE under (a) 350 nm and (b) 450 nm irradiation. 0.5 M Na_2SO_4 was used as electrolyte solution; irradiation from the back side.

10. References

(1) Grigioni, I.; Stamplecoskie, K. G.; Selli, E.; Kamat, P. V. Dynamics of Photogenerated Charge Carriers in WO_3/$BiVO_4$ Heterojunction Photoanodes. *J. Phys. Chem. C* **2015**, *119*, 20792–20800.

(2) Su, J.; Guo, L.; Yoriya, S.; Grimes, C. A. Aqueous Growth of Pyramidal-Shaped $BiVO_4$ Nanowire Arrays and Structural Characterization: Application to Photoelectrochemical Water Splitting. *Cryst. Growth Des.* **2010**, *10*, 856–861.

(3) Chen, Z.; Jaramillo, T. F.; Deutsch, T. G.; Kleiman-Shwarsctein, A.; Forman, A. J.; Gaillard, N.; Garland, R.; Takanabe, K.; Heske, C.; Sunkara, M.; et al. Accelerating Materials Development for Photoelectrochemical Hydrogen Production: Standards for Methods, Definitions, and Reporting Protocols. *J. Mater. Res.* **2011**, *25*, 3–16.

(4) Brida, D.; Manzoni, C.; Cirmi, G.; Marangoni, M.; Bonora, S.; Villoresi, P.; De Silvestri, S.; Cerullo, G. Few-optical-cycle Pulses Tunable from the Visible to the Mid-infrared by Optical Parametric Amplifiers. *J. Opt.* **2010**, *12*, 013001.

(5) Cerullo, G.; Manzoni, C.; Lüer, L.; Polli, D. Time-resolved Methods in Biophysics. 4. Broadband Pump–Probe Spectroscopy System with sub-20 fs Temporal Resolution for the Study of Energy Transfer Processes in Photosynthesis. *Photochem. Photobiol. Sci.* **2007**, *6*, 135–144.

(6) Ravensbergen, J.; Abdi, F. F.; Van Santen, J. H.; Frese, R. N.; Dam, B.; Van de Krol, R.; Kennis, J. T. M. Unraveling the Carrier Dynamics of $BiVO_4$: a Femtosecond to Microsecond Transient Absorption Study. *J. Phys. Chem. C* **2014**, *118*, 27793–27800.

(7) Kay, A.; Cesar, I.; Grätzel, M. New Benchmark for Water Photooxidation by Nanostructured α-Fe_2O_3 Films. *J. Am. Chem. Soc.* **2006**, *128*, 15714–15721.